2.6 FIRST INTERACTIVE SIMULATIONS OF CIRRUS CLOUDS FORMED BY HOMOGENEOUS FREEZING IN THE ECHAM GCM

Ulrike Lohmann[1,*] and Bernd Kärcher[2]
1: Dalhousie University, Halifax, Nova Scotia, Canada. 2: DLR Institute for Atmospheric Physics, Germany.

1. INTRODUCTION

The formation of ice in the atmosphere has long been recognized as a topic of great importance due to its key role in the precipitation process. While supersaturations with respect to ice in excess of 40% are necessary to freeze sulfate haze droplets, far lower supersaturations are needed for heterogeneous freezing of efficient ice nuclei.

Jensen et al. (1998) observed large ice particle number concentrations in wave-clouds with temperatures of about -37° C. They suggested that these ice crystals are caused by the activation of sulfate aerosols in liquid droplets followed by subsequent homogeneous freezing. At colder temperatures ($T < -60^\circ$ C) high supersaturations with respect to ice are also consistent with theoretical and laboratory studies suggesting that large supersaturations are required to homogeneously freeze sulfate aerosols. Koop et al. (2000) found that homogeneous freezing is independent of the chemical nature of the solution but only depends on the water activity of the solution droplets. The water activity of aerosol droplets in the atmosphere, in turn, is largely controlled by the relative humidity.

These findings were used in the parameterization of homogeneous freezing by Kärcher and Lohmann (2002). The parameterization was derived from first principles, building on the supersaturation and ice crystal growth equations. In contrast to previous parameterizations, this scheme considers the basic physical processes that eventually determine the number of ice crystals N_i forming during an adiabatic ascent, including the dependences of N_i on temperature and updraft speed. In particular, it was found that the number of crystals in young cirrus clouds, formed via homogeneous freezing of aqueous solution droplets, is quite insensitive to details of the aerosol size distribution in many cases, but increases rapidly with updraft velocity and decreases with temperature.

* *Corresponding author's address:* Ulrike Lohmann, Dept. of Physics and Atmospheric Science, Dalhousie Univ., Halifax, N.S. B3H 3J5, Canada; e-mail: Ulrike.Lohmann@Dal.Ca, URL: http://www.atm.dal.ca/~lohmann

2. MODEL DESCRIPTION

The ECHAM4 model used here is described in Lohmann and Kärcher (2002). Prognostic aerosol variables are mass mixing ratios of sulfate, hydrophilic and hydrophobic organic carbon, hydrophilic and hydrophobic black carbon, sub- and supermicron dust, and sub- and supermicron sea salt. The total number of hygroscopic aerosols N_a, that is used as the upper bound for the number of homogeneously frozen haze droplets N_i, is obtained by assuming an externally mixed aerosol. Prognostic cloud variables are mass mixing ratios of cloud liquid water and cloud ice and the number concentrations of cloud droplets and ice crystals. Cloud cover is diagnosed from relative humidity following Sundqvist et al. (1989). In order to get rid of the saturation adjustment scheme, the parameterization of the depositional growth of ice crystals by homogeneous and heterogeneous nucleation Q_{dep} (kg kg^{-1} s^{-1}) has been adopted from the mesoscale model GESIMA (Levkov et al. 1992) in the simulation HOM:

$$Q_{dep} = \left(\frac{\partial q_i}{\partial t}\right)_{dep} = 4\pi C A_T f_{Re}(S_i - 1)N_i \qquad (1)$$

where q_i is the ice water mixing ratio, C is the capacitance of an ice crystal evaluated as a spherical particle such that $C = D_i/2$, where D_i is the particle diameter; f_{Re} is the ventilation factor as a function of the Reynolds number, S_i is the saturation ratio over ice at the beginning of the time step, N_i is the ice crystal number concentration, and A_T is a thermodynamic function depending on pressure and temperature.

In simulation HOM, the number of newly frozen ice crystals at temperatures below -35° C is obtained from the parameterization by Kärcher and Lohmann (2002):

$$N_i^{hom} = min\left[\frac{m_w}{\rho_i}\left(\frac{b_2}{2\pi b_1}\right)^{\frac{3}{2}}\frac{a_1 S_{cr}}{a_2 + a_3 S_{cr}}\frac{w}{\sqrt{\tau}}; N_a\right] \qquad (2)$$

where m_w is the molecular weight of water, ρ_i is the ice crystal density ($= 925$ kg m^{-3}), S_{cr} is the critical supersaturation where freezing commences, w is the updraft velocity, $\tau \propto 1/w$ is the characteristic time scale of the nucleation event and $a_1, a_2 = 1/N_{si}, a_3, b_1 \propto N_{si}(S_{cr} - 1), b_2$ are temperature-dependent variables

explained in Kärcher and Lohmann (2002). Finally, $N_{si}(T)$ denotes the water vapor number density at ice saturation. Recall that the nucleation rate is limited by the number of hygroscopic aerosol particles N_a. As shown in Kärcher and Lohmann (2002), one can deduce the approximate scaling relationship

$$N_i^{hom} \propto w^{3/2} N_{si}^{-1/2}(T) \qquad (3)$$

where the mesoscale updraft velocity w is obtained as the sum of the grid mean vertical velocity and a turbulent contribution. In simulation HOM the number of newly formed ice crystals in the temperature range between 0 and -35° C is obtained from the parameterization of heterogeneous deposition-condensation freezing by Meyers et al. (1992):

$$N_i^{het} = \exp\,(\,-0.639 + 0.1296\,S_i) \qquad (4)$$

In the reference simulation (REF) neither the parameterization of heterogeneous deposition-condensation freezing (4) nor the parameterization of homogeneous freezing (2) is used. In REF the cirrus cloud water content is obtained using a saturation adjustment scheme from which the number of newly formed ice crystals is obtained.

3. COMPARISON WITH OBSERVATIONS

The simulations REF and HOM were conducted in T30 horizontal resolution with 19 vertical levels over a period of 3 years after an initial spin-up of 3 months using climatological sea surface temperatures. First we evaluate ECHAM's ability to simulate supersaturations with respect to ice. As the reference simulation does not allow any ice supersaturation at temperatures below -35° C, we use simulation HOM that includes the new cirrus parameterization of homogeneous freezing of solution droplets.

Gierens et al. (1999) analyzed three years of MOZAIC (measurement of ozone on Airbus in-service aircraft) measurements and derived a distribution law for the relative humidity in the upper troposphere and lower stratosphere. They determined the frequency distribution of relative humidity with respect to water and ice for stratospheric and tropospheric air in two layers centered around 200 and 250 hPa for cloud free conditions. We also extracted relative humidity with respect to ice (RH_i) from one year of ECHAM data for cloud free pixels in the same two layers as shown in Figure 1. We limited the data to the North Atlantic flight corridor (30° N to 90° N and 80° W to 0°) where most of the MOZAIC data were taken.

The MOZAIC data of RH_i decrease exponentially with increasing relative humidities above 100% very similar to what is seen in ECHAM. The slope describing the decrease in frequency of relative humidity between 119 and 148% in 200 hPa is the same in ECHAM as in the MOZAIC data. It is, however, lower than observed in 250 hPa. Here ECHAM predicts high relative humidities in excess of 130% more often than observed. This could have two reasons. The subgrid-scale vertical velocity could be too low, so that not enough ice crystals are formed and the ice crystals are not numerous enough for sufficient water vapor molecules to deposit onto them. Recall the strong dependence of N_i^{hom} on w as expressed in (3). On the other hand, the discrepancy between more frequently simulated high RH_i than observed could point to heterogeneous nucleation as one important mechanism that is currently lacking in our description of cirrus formation.

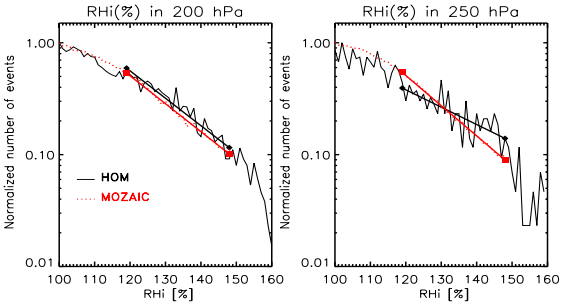

Figure 1: Normalized frequency distribution of relative humidity with respect to ice in two layers centered around 200 and 250 hPa for cloud free conditions from MOZAIC observations and simulation HOM together with average slopes between 119-148% RH_i.

Figure 2 shows annual zonal mean latitude versus pressure cross sections of specific and relative humidity, cloud cover and ice water mixing ratio, and ice crystal number concentrations for the simulations REF and HOM. Here the relative humidity is a hybrid of relative humidity with respect to water at temperatures above 273.2 K, with respect to ice at temperatures below 238.2 K, and a mixture of these two for temperatures between 238.2 and 273.2 K depending on the presence of ice clouds.

The relative humidity has maxima near the surface, in the polar regions, and in the upper tropical troposphere. The upper zonal mean maxima are increased in HOM to above 130% below the tropical and polar tropopause caused by the increase in specific humidity. ECHAM both simulates excessive water vapor at higher altitudes of the polar regions causing the hygropause to be too high (B. Steil, personal comm., 2001) and ECHAM has a cold bias in the polar upper troposphere (Roeckner et al. 1996). This model artifact has been amplified in HOM now that deposition does not set in at 100% RH_i and the relative humidity has increased by

up to 50%.

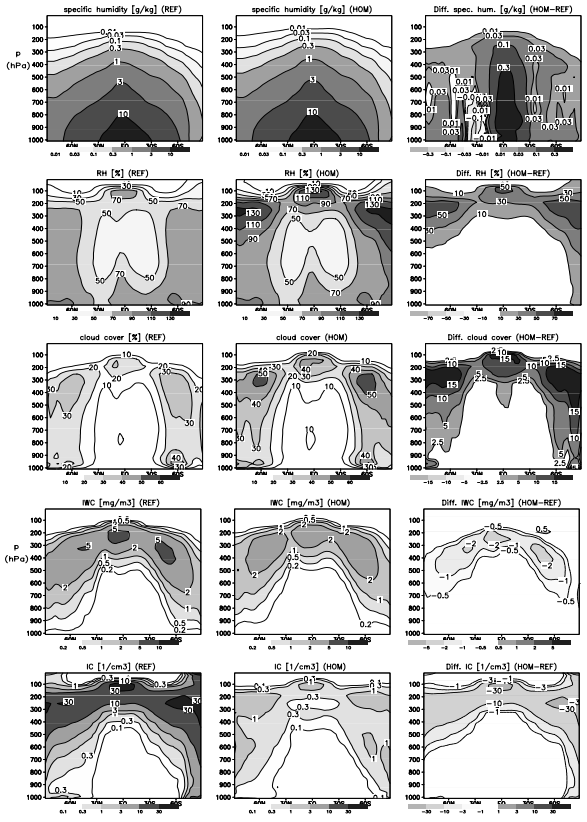

Figure 2: Annual zonal mean latitude versus pressure cross sections of specific humidity (g kg^{-1}), relative humidity (RH) (%), cloud cover (%), ice water content (mg m^{-3}) and ice crystal number concentrations (cm^{-3}) for the simulations REF, HOM and the difference HOM-REF.

Likewise the cloud cover is higher in these regions. This increase in cloud cover would lead to an increase in longwave cloud forcing. Since we constrain the model to match the observed global annual mean longwave and shortwave cloud forcing from ERBE, we enhanced the aggregation rate of ice particles into snow by a factor of 3, resulting in a faster removal of water from the atmosphere. As a consequence of increasing the aggregation rate, the ice water content is reduced in HOM as compared to REF. At the same time the number of ice crystals has decreased in HOM everywhere by roughly an order of magnitude. The maximum zonal mean concentrations of at least 1 cm^{-3} in HOM are located in the upper tropical and polar troposphere.

The comparison of annual zonal means of cloud cover and net cloud forcing with observations is shown in Figure 3. Most noticeably total cloud cover and especially high cloud cover has increased significantly in HOM as compared to REF. Whereas the increase in the tropics is in better agreement with the observations, the increase in extratropical high clouds caused by the increase in specific humidity is not supported by observations. Note that cloud cover and cloud water content are not consistently treated in ECHAM. That is, cloud cover depends only on relative humidity but is independent of the cloud water content.

The ice water path has decreased everywhere in HOM due to the faster aggregation rate. The net cloud forcing is very similar in both simulations. It is more negative than observed at the equator caused by excessive liquid water detrained from shallow convection (Lohmann, 2002). A common feature in many GCMs including ECHAM is a too small shortwave cloud forcing over mid-latitude oceans causing the net cloud forcing to be too small.

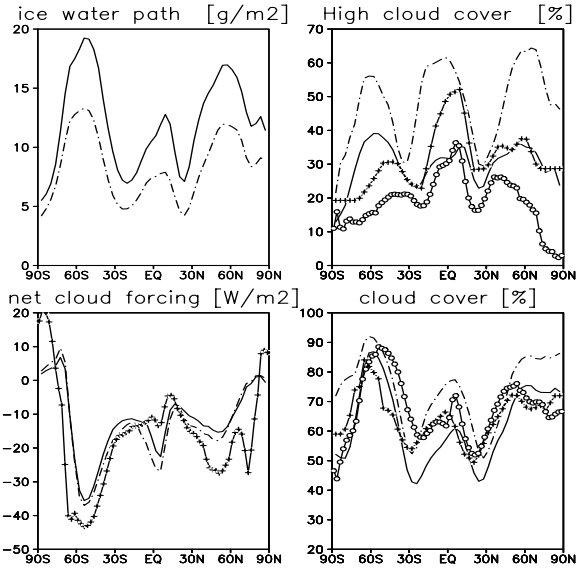

Figure 3: Annual zonal means of ice water path (g m^{-2}), high level cloud cover (%), total cloud cover (%) and net cloud forcing (W m^{-2}) for the simulations REF (solid line), HOM (dot-dashed line), and observations. Observations for high cloud cover are SAGE data (+) and ISCCP-D2 (o); for total cloud cover the data are surface observations (+) and ISCCP-D2 (o), and cloud forcing is from ERBE (+).

4. SUMMARY AND OUTLOOK

In this paper, we introduced the novel parameterization for homogeneous ice nucleation developed by Kärcher and Lohmann (2002) in the ECHAM GCM and performed the first interactive simulations of cirrus clouds in a global climate model. The main results of our study are as follows:

1. The formation and frequency of occurrence of cirrus clouds formed by homogeneous freezing of super-

cooled liquid aerosol particles is controlled by the vertical velocity and the temperature in the grid box and in some cases by the number of hygroscopic aerosols. The number of cirrus ice crystals formed in this way increases with increasing vertical velocity and decreasing temperature.

2. Assuming homogeneous freezing for all simulated types of particles below -35° C in the upper troposphere, anthropogenic changes of the hygroscopic aerosol concentration (e.g., of the abundance of sulfates and carbonaceous aerosols) does not result in a significant impact on cirrus cloud radiative properties but may determine ice crystal number concentrations in cirrus. The latter may be an artifact because we use a simplified bulk approach but no detailed aerosol microphysics. Thus, emissions of Aitken mode sulfate particles from aviation are unlikely to change the properties of cirrus clouds. Aircraft soot emissions will be important if the soot particles nucleate more efficiently than by homogeneous freezing.

3. The comparison with data taken on commercial aircraft (MOZAIC) showed that ECHAM reproduces the frequency distribution of supersaturation with respect to ice in cloud free regions well especially if high values of the subgrid scale vertical velocity are assumed (not shown). On the other hand, the higher frequency of occurrence of high supersaturations in the model may point to heterogeneous freezing as a missing mechanism for ice formation in the upper troposphere.

In a next step, we will generalize our analytic parameterization of homogeneous freezing to include aerosol size effects on cloud formation. Incorporating the refined parameterization into ECHAM will enable us to re-assess our results using a more realistic description of cirrus formation as well as to investigate the effects of enhanced sulfate aerosol levels caused by strong volcanic eruptions on the properties of high ice clouds (Sassen et al. 1992).

References

Gierens, K., Schumann, U., Helten, M., Smit, H. and Marenco, A. 1999. A distribution law for relative humidity in the upper troposphere and lower stratosphere derived from three years of MOZAIC measurements. *Ann. Geophysicae* **17**, 1218–1226.

Jensen, E. J., Toon, O. B., Tabazadeh, A., Sachse, G. W., Anderson, B. E., Chan, K. R., Twohy, C. W., Gandrud, B., Aulenbach, S. M., Heymsfield, A., Hallett, J. and Gary, B. 1998. Ice nucleation processes in upper tropospheric wave-clouds observed during SUCCESS. *Geophys. Res. Lett* **25**, 1363–1366.

Kärcher, B. and Lohmann, U. 2002. A parameterization of cirrus cloud formation: Homogeneous freezing of supercooled aerosols. *J. Geophys. Res.* **107**, 10.1029/2001JD000470.

Koop, T., Luo, B., Tsias, A. and Peter, T. 2000. Water activity as the determinant for homogeneous ice nucleation in aqueous solutions. *Nature* **406**, 611–614.

Levkov, L., Rockel, B., Kapitza, H. and Raschke, E. 1992. 3D mesoscale numerical studies of cirrus and stratus clouds by their time and space evolution. *Beitr. Phys. Atmos.* **65**, 35–58.

Lohmann, U. 2002. Possible aerosol effects on ice clouds via contact nucleation. *J. Atmos. Sci.* **59**, 647–656.

Lohmann, U. and Kärcher, B. 2002. First interactive simulations of cirrus clouds formed by homogeneous freezing in the ECHAM GCM. *J. Geophys. Res.* In press.

Meyers, M. P., DeMott, P. J. and Cotton, W. R. 1992. New primary ice-nucleation parameterization in an explicit cloud model. *J. Appl. Meteorol.* **31**, 708–721.

Roeckner, E., Arpe, K., Bengtsson, L., Christoph, M., Claussen, M., Dümenil, L., Esch, M., Giorgetta, M., Schlese, U. and Schulzweida, U. 1996. The atmospheric general circulation model ECHAM4: Model description and simulation of the present day climate. *Tech. Rep.* **218**, Max–Planck–Inst. für Meteorol., Hamburg, Germany.

Sassen, K. 1992. Evidence for liquid-phase cirrus cloud formation from volcanic aerosols: Climate implications. *Science* **257**, 1357–1369.

Sundqvist, H., Berge, E. and Kristiansson, J. E. 1989. Condensation and cloud parameterization studies with a mesoscale numerical weather prediction model. *Mon. Weather Rev.* **117**, 1641–1657.